R e s e a r c h a r t i c l e

urn:lsid:zoobank.org:pub:D063C3C3-76CD-450A-AC01-0035CFA51379

Taxonomic revision of the genus *Elmomorphus* Sharp, 1888 I. Japanese and Korean species (Coleoptera: Dryopidae)

Ján KODADA [1,*], Dávid SELNEKOVIČ [2], Manfred A. JÄCH [3],
Katarína GOFFOVÁ [4] & Peter VĎAČNÝ [5]

[1,2,4,5] Department of Zoology, Faculty of Natural Sciences, Comenius University in Bratislava,
Mlynská dolina B-1, SK-842 15 Bratislava, Slovakia.
[3] Naturhistorisches Museum Wien, Burgring 7, A–1010 Wien, Austria.

[*] Corresponding author: jan.kodada@uniba.sk
[2] Email: david.selnekovic@uniba.sk
[3] Email: manfred.jaech@nhm-wien.ac.at
[4] Email: katarina.goffova@uniba.sk
[5] Email: peter.vdacny@uniba.sk

[1] urn:lsid:zoobank.org:author:6E88BFBB-8769-44EC-8285-29E357CEC064
[2] urn:lsid:zoobank.org:author:D930D757-D929-4248-A29C-A857E0505345
[3] urn:lsid:zoobank.org:author:D749707A-8823-4110-8D51-BF5AF4E2820F
[4] urn:lsid:zoobank.org:author:4AE3FEFE-E697-43CE-844B-25609A9C0DB1
[5] urn:lsid:zoobank.org:author:47A28E80-E04F-40C4-93A3-F7F685C9533A

Abstract. The species of *Elmomorphus* Sharp, 1888 occurring in Japan and Korea are redescribed and illustrated: *E. brevicornis* Sharp, 1888 (Japan, Korea) and *E. amamiensis* Nomura, 1959 (Japan). The standard barcoding fragment of the mitochondrial gene coding for cytochrome *c* oxidase subunit I (COI) was sequenced and used together with morphological characters to delimit the taxonomic boundaries of the two species. To assess their morphometric variation, eight morphometric characters were measured and statistically evaluated using principal component analysis. The two species of *Elmomorphus* formed distinct and well-separated clusters in the COI tree. Their interspecific divergence is very high, ranging from 22.7 to 23.9%. On the other hand, morphometric characters, including those previously presumed to be diagnostic, overlap and per se do not allow unambiguous species identification. Reliable morphological distinguishing characters are described for males and females. Molecular data along with the morphological evidence strongly confirm the species status of *E. amamiensis*. An identification key to the Japanese and Korean species is provided.

Keywords. Long-toed water beetles, COI barcoding, integrative taxonomy.

Introduction

The genus *Elmomorphus* Sharp, 1888 was described by the renowned British coleopterist David Sharp (1840–1922) based on *E. brevicornis* Sharp, 1888 from Japan. Over the next 130 years, another 17 species were added, mainly from the Oriental Region.

The species of the genus *Elmomorphus* are regarded as True Water Beetles (Jäch 1998; Jäch & Balke 2008). They spend most of their life span submerged in various running water habitats. Most species prefer streams and rivulets flowing through forested areas. Immature adults undertake dispersal flights and are often collected in large numbers at light, at least the widely distributed and common species in Southeast Asia. However, there are numerous undescribed species, especially those living in primary rainforests (e.g., in Borneo), which were never collected at light, even if light traps were exposed near streams inhabited by large *Elmomorphus* populations.

Concerning the fauna of Japan, the family Dryopidae Billberg, 1820 is represented by four species: *Elmomorphus brevicornis* Sharp, 1888 (type species), *E. amamiensis* Nomura, 1959, *Helichus ussuriensis* Lafer, 1980 and the recently recorded and obviously introduced *Dryops nitidulus* (Heer, 1841) (Yoshitomi & Haga 2018; Nakajima *et al.* 2020). As for Korea, only one dryopid species, *E. brevicornis*, has been recorded so far (Jung & Bae 2014; Kodada & Jäch 2016).

Due to the remarkable morphological similarity, *E. amamiensis* was initially described as a subspecies of *E. brevicornis* by Nomura (1959) from Amami Island in the Ryukyu Archipelago. The specific status was proposed recently by Jung & Bae (2014), referring to several more or less evident morphological characters.

We examined the type material of *E. brevicornis* housed in the Sharp collection in the Natural History Museum London and additional material, including freshly collected specimens of both taxa from Japan. Using an integrative taxonomic approach, we redescribe, illustrate, and diagnose *E. brevicornis* and *E. amamiensis*, and provide reliable morphological distinguishing characters for both sexes.

This publication is the first part of a comprehensive taxonomic revision of the genus *Elmomorphus*. The second part (in prep.) will deal with the Chinese species, and it will include a thorough morphological redescription of the genus. The final parts will deal with the species of the Oriental and Australian regions. The revision of *Elmomorphus* started in the 1990s, but due to the ever-growing number of specimens and new species collected, its publication has been retarded.

Material and methods

Taxonomic methods

The material examined in this study is deposited in the Natural History Museum London, United Kingdom (NHMUK), Naturhistorisches Museum Wien, Austria (NHMW), and the Ján Kodada collection, Comenius University in Bratislava, Slovakia (JKCB).

Dry specimens were firstly relaxed for several hours in water with several drops of concentrated acetic acid. Male genitalia were dissected, cleared in lactic acid for one or two days, and temporarily mounted on a microscope slide with a single cavity in Berlese's fluid (Swan 1936). After examination/drawing, the male genitalia were mounted in a drop of DMHF on the same card as the respective specimen. Female genitalia were observed in glycerol and stored in micro-vials filled with glycerol and pinned under the studied specimen. Examination and dissection were made under a Leica MZ16 stereo microscope with magnifications up to 120× and a diffuse LED lighting. Drawings were hand-made with a pencil, using a drawing device attached to a Leica DM 1000 microscope and subsequently traced in Adobe

Illustrator CC. The specimens were photographed under a Zeiss Axio-Zoom V-16 stereo microscope and a Canon 5D Mark IV camera attached. Each habitus photography was created by stacking 100–120 focal planes using the software ZereneStacker (https://zerenesystems.com/cms/stacker).

For scanning electron microscopy, specimens were dehydrated in graded ethanol series and air-dried from absolute ethanol, coated with gold, and then viewed in a TESCAN microscope.

Label data are cited verbatim, enclosed within quotation marks; individual labels are separated by a vertical bar; square brackets enclose additional information.

The morphological terminology is primarily based on Kodada *et al.* (2016) with some additions.

Measurements were made under a Leica MZ16 stereo microscope with Leica eyepiece cross micrometre (5 : 100). In total, 12 morphometric characters, as listed in the 'Abbreviations' section below, were scored on 37 specimens. The range of measured values and ratios is followed by mean, standard deviation, and the number of individuals measured.

Principal component analysis (PCA) was conducted on eight morphometric characters: PL, PW, EL, EW, PrTL, MsTL, MtTL, and ID. Datasets were compiled separately for both sexes and included 14 males and seven females of *E. brevicornis*, and nine males and seven females of *E. amamiensis*. Data were log-transformed before the analysis, and a variance-covariance matrix was used for the subsequent calculations. Several specimens used for DNA isolation were also included in the datasets. The analysis was performed in the PAST 3.12 software (Hammer *et al.* 2001). Plots were edited in Adobe Illustrator CC.

Molecular methods

Eight specimens of *E. amamiensis* and 16 specimens of *E. brevicornis* from Japan, fixed in 96% ethanol were used for molecular analyses. Unfortunately, no specimens from Korea were available. Tissue samples contained either one leg with coxa and attached muscle, or the entire abdomen of an adult specimen. DNA was isolated with the E.Z.N.A.® Tissue DNA kit (OMEGA Bio-tek Inc., Norcross, GA, USA) according to the manufacturer's protocol. The 5' end of the mitochondrial gene coding for cytochrome *c* oxidase subunit I (COI), the standard barcode (Hebert *et al.* 2003), was PCR amplified with the standard primers LCO1490 and HCO2198 (Folmer *et al.* 1994). Individual PCR reactions were conducted in a total volume of 15 μl and included 6.67 μl of GoTaq® Green master mix (Promega, Fitchburg, WI, USA), 0.34 μl of each primer (10 pmol/μl), 50 ng of template DNA, and 4.65 μl nuclease-free water. The PCR thermocycler program was as follows: 94°C for 180 s, 40 cycles of 94°C for 40 s, 52°C for 40 s, and 72°C for 60 s, and 72°C for 10 min. PCR products were extracted from the 1% TBE agarose gel, using the Exo-CIP™ Rapid PCR Cleanup Kit (New England Biolabs® Inc., Ipswich, MA, USA) according to the manufacturer's protocol. Purified PCR products were sequenced from both sides in Macrogen Europe B.V. (Amsterdam, Netherlands). Sequences were trimmed and assembled into contigs in Geneious ver. 6.1.8 (https://www.geneious.com).

Phylogenetic methods

The nucleotide COI sequences were aligned based on the predicted amino acid sequences with MEGA-X (Kumar *et al.* 2018), using the invertebrate mitochondrial genetic code and the MUSCLE codon algorithm. COI sequences of *Pomatinus substriatus* (Müller, 1806) and *Dryops auriculatus* (Geoffroy, 1785) were retrieved from the GenBank database (https://www.ncbi.nlm.nih.gov/genbank/) and served as outgroup. Their accession numbers are specified in the respective figure.

Three algorithms were used to infer phylogenetic relationships and to confirm the consistency of the results. A maximum likelihood tree was constructed with the program IQTree (Nguyen *et al.* 2015) on

XSEDE ver. 1.6.10, using the CIPRES science gateway ver. 3.3 (http://www.phylo.org/) (Miller *et al.* 2010). The best fitting evolutionary substitution model was determined with the aid of the BIC criterion, using the in-built ModelFinder program. The maximum likelihood analyses included the BioNJ tree option to build the starting tree, correction for ascertainment bias, 1000 ultrafast bootstrap replicates to assess the reliability of internal nodes, and the bnni algorithm to reduce overestimating support (Hoang *et al.* 2018). Bayesian inference was carried out in the program MrBayes (Ronquist *et al.* 2012) on XSEDE ver. 3.2.7 under the best evolutionary substitution model, as selected with the BIC criterion in jModelTest ver. 2.1.10 (Darriba *et al.* 2012). Markov Chain Monte Carlo (MCMC) simulations included two independent runs each with four simultaneous chains, one million generations, a sampling frequency of trees and parameters at one hundred, and a burn-in fraction at 25%. Convergence of the MCMC analyses to stationary distribution and an adequate sample from the posterior distribution were confirmed using the in-built MrBayes diagnostics. Finally, a distance neighbour-joining (NJ) tree was constructed with the maximum composite likelihood method, gamma distributed rates among sites ($\alpha = 0.5$), and heterogenous patterns among lineages. The reliability of nodes in the distance tree was assessed with 1000 bootstrap pseudo-replicates. All trees were computed as unrooted and were rooted a posteriori using the outgroup taxa in FigTree ver. 1.2.3 (http://tree.bio.ed.ac.uk/software/figtree/).

For the barcoding analyses, pairwise *p*-distances were calculated in MEGA-X (Kumar *et al.* 2018). Histograms showing the intraspecific, interspecific as well as the intergeneric distances were prepared in Python ver. 3.6.6, using the libraries scikit-learn (Pedregosa *et al.* 2011) and Matplotlib (Hunter 2007). Multidimensional scaling (MDS) was carried out on the pairwise *p*-distances with the scikit-learn library. The ordination MDS diagram was constructed with the metric technique, the SMACOF algorithm, and 250 initializations, whereby each initialization had 20 000 iterations, and ε was set to 10^{-8} to declare convergence.

A haplotype network was calculated from the COI alignment using the TCS method (Clement *et al.* 2000) in PopART ver. 1.7 (Leigh & Bryant 2015). Mutations were displayed as numbers along the network edges.

Abbreviations

APD = linear distance between anterior angles of pronotum in dorsal aspect
EL = elytral length from the middle of the anterior margin of the scutellum (scutellary shield) to the apex of the elytra
EW = greatest width of elytra in dorsal aspect
ID = minimum linear distance between eyes in dorsal aspect
MsTL = maximum length of mesotibia
MtTL = maximum length of metatibia
PhL = greatest linear distance between base and apex of phallobase in the lateral aspect
PL = pronotal length along the midline
PrL = greatest linear distance between base and apex of parameres in the lateral aspect
PrTL = maximum length of protibia
PW = maximum pronotal width
TL = linear distance between the anterior margin of the pronotum and the apex of the elytra along the midline

Results

Phylogenetic analyses

Nineteen new COI sequences were obtained from two species of *Elmomorphus*; seven sequences from *E. amamiensis* and 12 sequences from *E. brevicornis*. Their origin and GenBank accession numbers are

Table 1. Origin and GenBank accession numbers of COI sequences used in phylogenetic analyses.

Sample code	Locality	GenBank no.
*Elmomorphus amamiensis*_JK217	JAPAN, Kagoshima Pref., Amami Island	MW036754
*Elmomorphus amamiensis*_JK218	JAPAN, Kagoshima Pref., Amami Island	MW036755
*Elmomorphus amamiensis*_JK220	JAPAN, Kagoshima Pref., Amami Island	MW036756
*Elmomorphus amamiensis*_JK221	JAPAN, Kagoshima Pref., Amami Island	MW036757
*Elmomorphus amamiensis*_JK222	JAPAN, Kagoshima Pref., Amami Island	MW036758
*Elmomorphus amamiensis*_JK223	JAPAN, Kagoshima Pref., Amami Island	MW036759
*Elmomorphus amamiensis*_JK224	JAPAN, Kagoshima Pref., Amami Island	MW036760
*Elmomorphus brevicornis*_JK226	JAPAN, Shimane Pref., Matsue, Yakumo	MW036761
*Elmomorphus brevicornis*_JK227	JAPAN, Shimane Pref., Matsue, Yakumo	MW036762
*Elmomorphus brevicornis*_JK228	JAPAN, Shimane Pref., Matsue, Yakumo	MW036763
*Elmomorphus brevicornis*_JK229	JAPAN, Shimane Pref., Matsue, Yakumo	MW036764
*Elmomorphus brevicornis*_JK230	JAPAN, Shimane Pref., Matsue, Yakumo	MW036765
*Elmomorphus brevicornis*_JK231	JAPAN, Shimane Pref., Matsue, Yakumo	MW036766
*Elmomorphus brevicornis*_JK232	JAPAN, Shimane Pref., Matsue, Yakumo	MW036767
*Elmomorphus brevicornis*_JK233	JAPAN, Shimane Pref., Izumo, Nishitani	MW036768
*Elmomorphus brevicornis*_JK234	JAPAN, Shimane Pref., Izumo, Nishitani	MW036769
*Elmomorphus brevicornis*_JK235	JAPAN, Shimane Pref., Izumo, Nishitani	MW036770
*Elmomorphus brevicornis*_JK236	JAPAN, Shimane Pref., Izumo, Nishitani	MW036771
*Elmomorphus brevicornis*_JK237	JAPAN, Shimane Pref., Izumo, Nishitani	MW036772
Pomatinus substriatus	GERMANY, Bavaria, Isen River near Oberdorfen	KM445386.1
Pomatinus substriatus	FRANCE, Durance River	MF458799.1
Dryops auriculatus	GERMANY, Saxony-Anhalt, Huy north of Athenstedt	KU906802.1
Dryops auriculatus	GERMANY, Saxony-Anhalt, Huy north of Athenstedt	KU918229.1

summarised in Table 1. Three phylogenetic methods (IQTree, MrBayes, and NJ) were utilised to delimit their taxonomic boundaries and reconstruct their interrelationships. All algorithms brought almost identical results and, therefore, only the maximum likelihood IQTree is presented along with nodal supports from all three statistical methods (Fig. 1A). The two species of *Elmomorphus* formed strongly to fully statistically supported clusters that were separated by long branches in the COI trees. Despite their deep divergence, *E. amamiensis* and *E. brevicornis* grouped with very strong statistical support (98% IQTrees, 1.00 MrBayes, 97% NJ). Their monophyletic origin was recognized not only when the trees were rooted by outgroup taxa, but also when the midpoint rooting method was applied.

The distinctness as well as the deep divergence of the two species of *Elmomorphus* were also corroborated by barcoding analyses and multidimensional scaling. The intraspecific distances ranged from 0.0 to 0.5% within *E. amamiensis* and from 0.0 to 2.1% within *E. brevicornis* (Table 2). There was no overlap between intraspecific and interspecific *p*-distances, but interspecific and intergeneric distances significantly overlapped in the histogram (Fig. 1B). This pattern was caused by the very deep interspecific divergence of *E. amamiensis* and *E. brevicornis*, which spanned a range of 22.7–23.9% (Table 2). Similarly, each species formed a homogenous cluster well separated from all other taxa in the MDS ordination diagram inferred from the pairwise *p*-distances (Fig. 1C). Distances among individual species were comparable, documenting their deep genetic divergences as well.

Haplotype network analyses supported the monophyletic origin of *E. amamiensis* and *E. brevicornis* by 55 shared nucleotide positions within the 567 nucleotides long barcoding COI sequence fragment. Specimens of the former species were separated by 1–3 mutation steps, while those of the latter species by 1–12 mutation steps. The two species of *Elmomorphus* differed by as many as 109 nucleotide positions, documenting their very deep genetic divergence (Fig. 2).
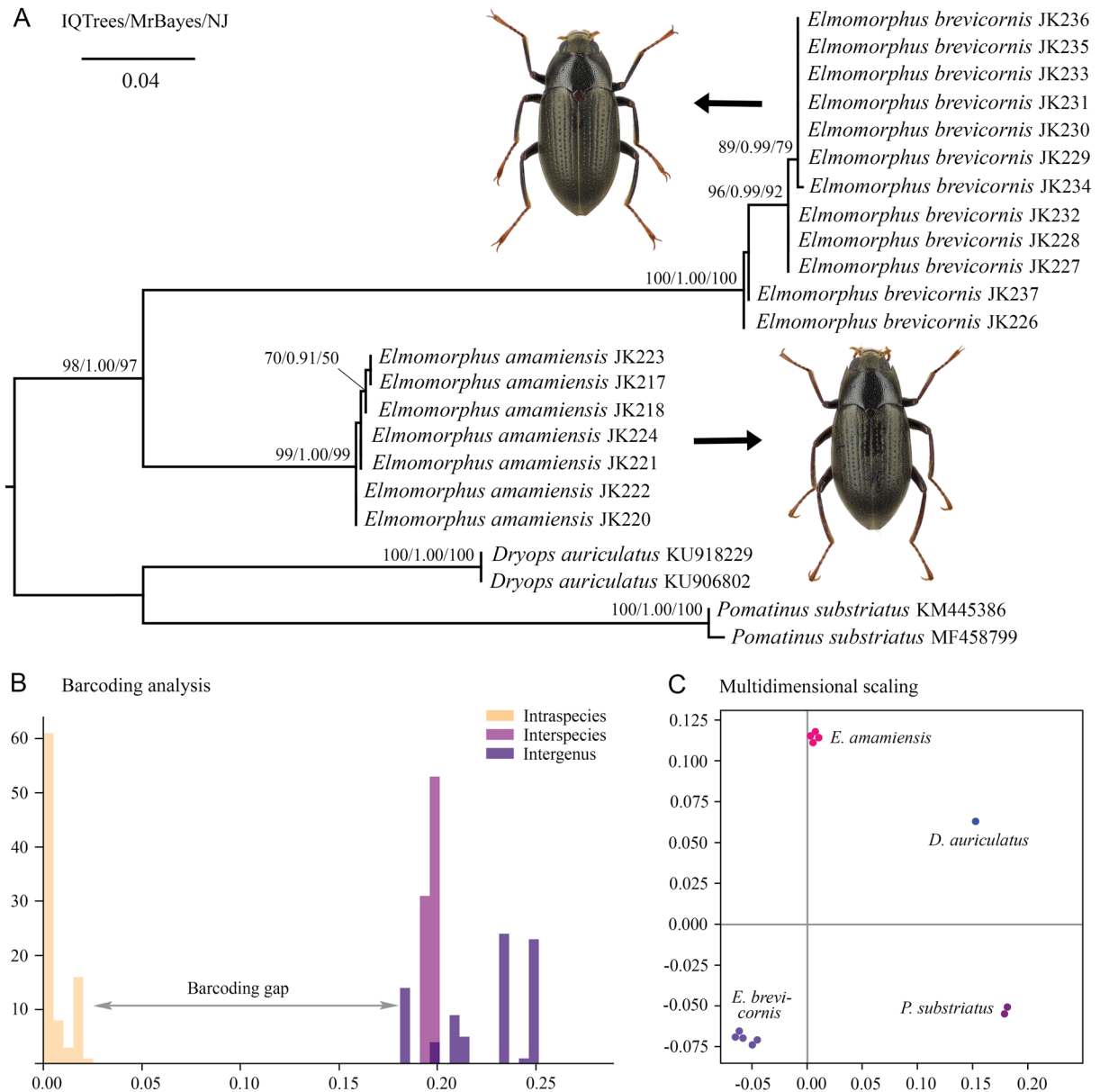

Fig. 1. Phylogenetic relationships and genetic distances between Japanese *Elmomorphus* species. *Pomatinus substriatus* (Müller, 1806) and *Dryops auriculatus* (Geoffroy, 1785) served as outgroup taxa in all analyses. **A**. Phylogenetic tree based on the mitochondrial COI gene. Bootstrap values for maximum likelihood analyses performed in IQTrees and distance NJ analyses performed in MEGA-X as well as posterior probabilities for Bayesian interference performed in MrBayes were mapped onto the best scoring IQTree. The scale bar denotes four substitutions per 100 nucleotide positions. **B**. Histogram displaying intraspecies, interspecies, and intrageneric distances of the taxa shown in (A). **C**. Multidimensional scaling based on *p*-distances of the taxa shown in (A).

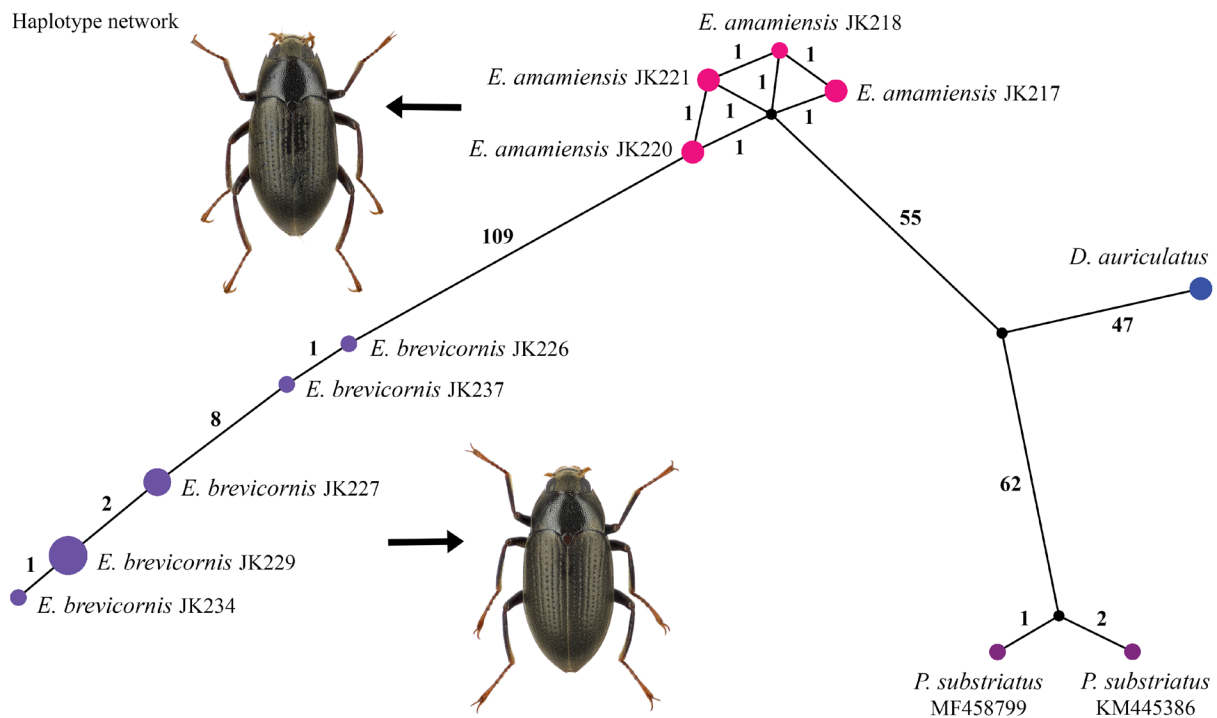**Table 2.** Pairwise *p*-distances of the COI fragment sequences of *Elmomorphus brevicornis* Sharp, 1888, *Elmomorphus amamiensis* Nomura, 1959 and outgroup taxa (shaded grey).

	JK217	JK218	JK220	JK221	JK222	JK223	JK224	JK226	JK227	JK228	JK229	JK230	JK231	JK232	JK233	JK234	JK235	JK236	JK237	KM445386.1	MF458799.1	KU906802.1
JK217_E. amamiensis																						
JK218_E. amamiensis	0.002																					
JK220_E. amamiensis	0.005	0.004																				
JK221_E. amamiensis	0.004	0.002	0.002																			
JK222_E. amamiensis	0.005	0.004	0.000	0.000																		
JK223_E. amamiensis	0.000	0.002	0.002	0.004	0.005																	
JK224_E. amamiensis	0.004	0.002	0.002	0.000	0.002	0.004																
JK226_E. brevicornis	0.229	0.232	0.227	0.229	0.227	0.229	0.229															
JK227_E. brevicornis	0.234	0.236	0.231	0.234	0.231	0.234	0.234	0.016														
JK228_E. brevicornis	0.234	0.236	0.231	0.234	0.231	0.234	0.234	0.016	0.000													
JK229_E. brevicornis	0.234	0.236	0.231	0.234	0.231	0.234	0.234	0.020	0.004	0.004												
JK230_E. brevicornis	0.234	0.236	0.231	0.234	0.231	0.234	0.234	0.020	0.004	0.004	0.000											
JK231_E. brevicornis	0.234	0.236	0.231	0.234	0.231	0.234	0.234	0.020	0.004	0.004	0.000	0.000										
JK232_E. brevicornis	0.234	0.236	0.231	0.234	0.231	0.234	0.234	0.020	0.004	0.004	0.000	0.000	0.000									
JK233_E. brevicornis	0.234	0.236	0.231	0.234	0.231	0.234	0.234	0.016	0.000	0.000	0.004	0.004	0.004	0.004								
JK234_E. brevicornis	0.236	0.239	0.234	0.236	0.234	0.236	0.236	0.020	0.004	0.004	0.000	0.000	0.000	0.000	0.002							
JK235_E. brevicornis	0.234	0.236	0.231	0.234	0.231	0.234	0.234	0.021	0.005	0.005	0.002	0.002	0.002	0.002	0.002	0.002						
JK236_E. brevicornis	0.234	0.236	0.231	0.234	0.231	0.234	0.234	0.020	0.004	0.004	0.000	0.000	0.000	0.000	0.000	0.000	0.000					
JK237_E. brevicornis	0.231	0.234	0.229	0.232	0.229	0.231	0.232	0.020	0.014	0.014	0.018	0.018	0.018	0.014	0.018	0.020	0.018	0.018				
KM445386.1_P. substriatus	0.250	0.250	0.251	0.248	0.251	0.250	0.248	0.302	0.307	0.307	0.307	0.307	0.307	0.307	0.307	0.308	0.307	0.307	0.307			
MF458799.1_P. substriatus	0.248	0.248	0.248	0.246	0.248	0.248	0.246	0.305	0.310	0.310	0.310	0.310	0.310	0.310	0.310	0.310	0.310	0.310	0.310	0.005		
KU906802.1_D. auriculatus	0.210	0.210	0.209	0.209	0.209	0.210	0.209	0.279	0.284	0.284	0.284	0.284	0.284	0.284	0.284	0.281	0.284	0.284	0.284	0.233	0.225	
KU918229.1_D. auriculatus	0.210	0.210	0.209	0.209	0.209	0.210	0.209	0.279	0.284	0.284	0.284	0.284	0.284	0.284	0.284	0.281	0.284	0.284	0.284	0.233	0.225	0.000

Multivariate morphometric analyses

To assess the morphometric variation of the two species, principal component analysis (PCA), based on eight morphometric characters, was carried out for each sex separately. In males, the first and second principal components (PC1 and PC2) explained 62.58% and 25.16% of the total variance, respectively. Two homogenous groups, each representing one species of *Elmomorphus*, were rather well separated along the first ordination axis (Fig. 3A). The pronotal length and width strongly correlated with PC1, while the length of meso- and metatibia with PC2 (Table 3). Thus, specimens with smaller bodies and longer tibiae are clustered in the upper left part of the ordination diagram, while individuals with larger bodies and shorter tibiae are placed in the lower right corner. These positions correspond well with raw measurements according to which the average body size of *E. amamiensis* males is smaller, while the tibiae of the males of *E. brevicornis* are on average longer. Although the average values are comparatively different, the character ranges overlap in the two species. Individual characters thus do not allow unambiguous identification. However, the combination of eight morphometric features can differentiate males of the two species without any overlap in the phenotypic space.

In females, PC1 and PC2 explained 77.92% and 8.93% of the total variance, respectively. Females of the two species of *Elmomorphus* were only vaguely separated along the first ordination axis, as two specimens of *E. brevicornis* were placed within the rather compact cluster of *E. amamiensis* individuals (Fig. 3B). The pronotal length and the elytral width strongly correlated with PC1, while the length of the protibia and the interocular distance correlated with PC2 (Table 3). The cluster of *E. brevicornis*

Fig. 2. TCS haplotype network of COI sequences of *Elmomorphus brevicornis* Sharp, 1888, *Elmomorphus amamiensis* Nomura, 1959 and two outgroup taxa. Numbers along edges represent mutational steps. For specimens belonging to individual haplotype groups, see Fig. 1A.

Table 3. Explained variance and loadings onto the first three principal components for males and females of *Elmomorphus brevicornis* Sharp, 1888 and *Elmomorphus amamiensis* Nomura, 1959. Loadings with first and second highest absolute values in each component are in boldface.

	males			**females**		
	PC 1	**PC 2**	**PC3**	**PC 1**	**PC 2**	**PC 3**
Explained variance (%)	62.58	25.16	4.70	77.92	8.93	5.48
Loadings:						
PL	**0.508**	0.207	-0.022	**0.495**	-0.059	**-0.839**
PW	**0.543**	-0.266	0.008	0.361	0.162	0.149
EL	0.389	-0.070	**-0.364**	0.344	0.052	0.169
EW	0.413	-0.241	-0.253	**0.406**	0.402	0.119
PrTL	0.124	0.441	0.006	0.386	**-0.464**	0.274
MsTL	0.096	**0.501**	-0.056	0.310	-0.225	0.097
MtTL	0.126	**0.613**	-0.021	0.247	-0.343	**0.326**
ID	0.291	-0.046	**0.894**	0.190	**0.650**	0.202

females showed a size gradient with the smallest specimens located in the left part of the ordination diagram, where they were mixed with *E. amamiensis* females. The present multivariate analyses show that females of the two species cannot be unambiguously differentiated even when a combination of eight morphometric characters is considered.
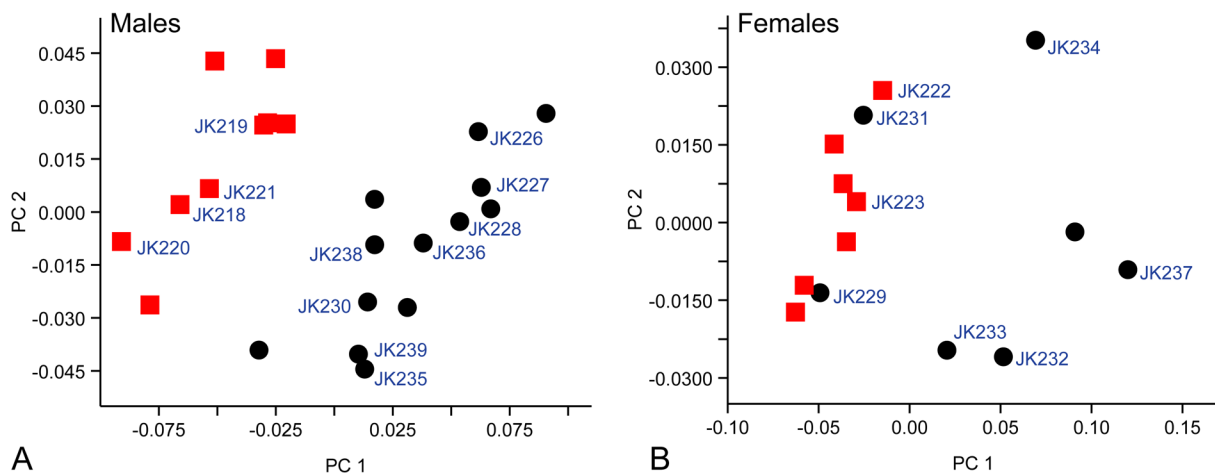
Fig. 3. Ordination of *Elmomorphus brevicornis* Sharp, 1888 (black circles) and *Elmomorphus amamiensis* Nomura, 1959 (red squares) along PC1 and PC2 axis. **A**. Males. **B**. Females.

Taxonomy

<div align="center">

Class Insecta Linnaeus, 1758
Order Coleoptera Linnaeus, 1758
Suborder Polyphaga Emery, 1886
Superfamily Byrrhoidea Latreille, 1804
Family Dryopidae Billberg, 1820
Genus *Elmomorphus* Sharp, 1888

Elmomorphus brevicornis Sharp, 1888
Figs 4A–C, 5A, 6A, C, E, 7A–D, 8A–B, E–F, 9A–B, D, 10A

</div>

Elmomorphus brevicornis Sharp, 1888: 243 (original description, type locality).
Helichus "862 spec. ?" Lewis 1879: 12 (first indication).

Elmomorphus brevicornis – Zaitzev 1910: 19 (catalogue). — Kôno 1934: 125 (catalogue). — Bollow 1940: 59–62, figs 271–276 (description, Japanese records). — Chûjô & Satô 1964: 193. — Delève 1968: 151 (differential diagnosis). — Satô 1981: 53. — Jäch 1984: 314 (checklist). — Kodada & Jäch 2006: 442 (catalogue). — Hayashi & Shimada 2006: 129 (Japanese records, in Japanese). — Yoshioka 2007: 236, 242, fig. 17a (Japanese records, in Japanese); 2008: 224 (Japanese records, in Japanese). — Hayashi 2011: 93. — Kamezawa & Nomura 2013: 29 (Japanese records, in Japanese). — Jung & Bae 2014: 2–7, figs 2a–c, 3–5 (description, identification key, Korean records). — Kodada & Jäch 2016: 606 (catalogue). — Yoshitomi & Haga 2018: 341–342 (identification key). — Nakajima *et al.* 2020: 177, 322 (diagnosis, identification key, photographs of living specimens).

non *Elmomorphus brevicornis* – Devi *et al.* 2016: 371–373 (misidentification, invalid lectotype designation)].

Type locality
Kobe, Hyōgo Prefecture, southern Honshu, Japan.

Material examined
Syntypes
JAPAN • 1 ♂ (Fig. 4C); "Kobe 18.V.71 [handwritten] | Japan. G Lewis 1910—320. [printed] | *Elmomorphus brevicornis* [handwritten] | *Elmomorphus brevicornis*. [handwritten] | *Elmomorphus brevicornis* Sharp det. H. Bollow 1934 [handwritten and printed]"; NHMUK • 1 ♀ (Fig. 4A–B); "*Elmomorphus brevicornis* Type D.S. [David Sharp] Jokio [sic]. Japan Lewis . [handwritten] | Japan. G.Lewis [printed] | Sharp Coll. 1905-313. [printed] | Type [printed, round label with red frame]"; NHMUK.

Additional material
JAPAN • 1 ♀; "Shimakatsu Mie-Pref. 16.XI.1958 Coll. Shozo Ishida | *Elmomorphus brevicornis* Sharp Det. M. SATO 1971"; NHMW • 1 ♂; "Nagara-River Gifu-City 26.VII.1951 Coll. Zen. Naruse"; NHMW • 1 ♂; "Kurokawa, N-Echigo 2.IX.1960 Col. K. Baba"; NHMW • 1 ♂; "Kabuchi-gawa Gifu Pref. 18.VIII.1967 M. Sato leg."; NHMW • 10 ♂♂, 6 ♀♀; "Japan, Shimane Pref.: Matsue: Yakumo 26.–30. iii.2019 M. Hayashi"; JKCB • 5 ♂♂, 3 ♀♀; "Japan, Shimane Pref.: Izumo, Nishitani 30.iii.2019 M. Hayashi"; JKCB • 1 ♀; "NE-JAPAN Miyagi Pr., Mts. Abukuma, 6.6. Uchikawa riv., leg. Ohmomo 1987 | *Elmomorphus brevicornis* Sharp"; NHMW.

SOUTH KOREA • 1 ♂, 1 spec. sex not examined; "South Korea, Jeollabuk-do, Buan-gun, Byeonsan-myeon, Junggye-ri, Jiko Falls 15.VI.2011, leg. S.W.Jung"; NHMW.

Note

The original description was based on two specimens collected by G. Lewis. Both specimens are still preserved in the collection of David Sharp in the NHMUK. The female specimen is glued on a larger rectangular card with the following handwritten text: "*Elmomorphus brevicornis* Type D.S. Jokio. Japan Lewis.". This style of labelling and label text is typical of David Sharp's type material. The male specimen and the dissected aedeagus are glued on one card, while its detached appendages are glued on a second card, pinned below the specimen. The two syntypes are conspecific. However, while the type locality mentioned in the original description ("Kobé") is written on the original label of the male specimen (Fig. 4C), the name "Jokio" [Sharp's spelling of Tokyo] is found on the label of the female specimen (Fig. 4A). Since no other species is known from Honshu and since taxonomic confusion is improbable, a lectotype designation is considered unnecessary (see ICZN 1999: Recommendation 74G, https://www.iczn.org/the-code/declaration-44-amendment-of-article-74-7-3/).

In the abstract of their most remarkable article, Devi *et al.* (2016: 371) wrote that "A lectotype is designated for this species [*Elmomorphus brevicornis*]". However, the term "lectotype" is not used anywhere else in their article, and it does not contain sufficient information to ensure recognition of the specimen designated. Therefore, the requirements of the International Code of Zoological Nomenclature (ICZN 1999: Art. 74.7) are not fulfilled.

Fig. 4. *Elmomorphus brevicornis* Sharp, 1888. **A–B**. Syntype, ♀ (NHMUK). **A**. Specimen glued on the original card with Sharp's handwriting. **B**. Labels. **C**. Syntype, ♂ (NHMUK), labels (the last label not depicted).

Diagnosis

Elmomorphus brevicornis is a medium-sized (TL 2.59–3.51 mm), elongated oval, dorsally moderately convex species, with the highest point at the anterior third of the elytral length (lateral view). Body outline discontinuous between pronotum and elytra; yellowish plastron microscales cover the entire surface of the cranium, lateral portions of the pronotum and the entire dorsal surface of the elytra, so most of the dorsal surface appears to be matt (Fig. 5A). Each elytron has nine rows of large round punctures arranged in shallow striae. Legs conspicuously long and robust, only moderately shorter than the combined length of pronotum and elytra.

Elmomorphus brevicornis closely resembles *E. amamiensis* in external morphology, and it can be distinguished by the following characteristics: (1) elytral sides in *E. brevicornis* subparallel in the anterior half, while in *E. amamiensis* they are arcuate and more convergent (Fig. 5B), thus the outline appears to be generally broader and less oval in *E. brevicornis*; (2) sides of pronotum usually more rounded in *E. brevicornis*, while they are almost straight in *E. amamiensis*; (3) males of *E. brevicornis* with several longer setae in a transverse row on the labrum, and with similar setae in two pairs of clusters on each prosternal process and on the admedian portions of metaventrite, row and clusters of setae rather inconspicuous (Fig. 6A, C, E); similar, longer setae also near the apex of the fifth ventrite (Fig. 7D); in the male of *E. amamiensis* the setal row and all setal clusters are well developed, conspicuous (Figs 6B, D, F, 7E); (4) parameres weakly curved ventrad in *E. brevicornis* (Fig. 8B), but strongly curved in *E. amamiensis* (Fig. 8D); (5) bursa copulatrix of the two species distally with one cluster of microspines on each side (Fig. 9D), while in *E. amamiensis,* besides these microspines there are several additional larger sclerites (Fig. 9E). Except for differences in the morphological characters, the two species differ by 22.7–23.9% in the partial mtDNA encoding for cytochrome *c* oxidase subunit I.

Measurements (mm)

TL: ♂♂ 2.89–3.38 (3.10 ± 0.13, n = 14), ♀♀ 3.15–3.51 (3.34 ± 0.12, n = 7); PL: ♂♂ 0.65–0.85 (0.78 ± 0.05, n = 14), ♀♀ 0.75–0.90 (0.83 ± 0.05, n = 7); PW: ♂♂ 1.20–1.43 (1.33 ± 0.06, n = 14), ♀♀ 1.30–1.47 (1.40 ± 0.06, n = 7); EL: ♂♂ 2.22–2.57 (2.42 ± 0.09, n = 14), ♀♀ 2.50–2.86 (2.66 ± 0.11, n = 7); EW: ♂♂ 1.44–1.66 (1.54 ± 0.05, n = 14), ♀♀ 1.51–1.77 (1.65 ± 0.09, n = 7); MsTL: ♂♂ 0.82–0.94 (0.88 ± 0.03, n = 14), ♀♀ 0.87–0.97 (0.91 ± 0.03, n = 7); MtTL: ♂♂ 0.91–1.09 (1.02 ± 0.05, n = 14), ♀♀ 0.97–1.12 (1.06 ± 0.05, n = 7); PhL: 0.73–0.89 (0.83 ± 0.04, n = 11); PrL: 0.32–0.39 (0.37 ± 0.02, n = 11).

Redescription

Body. Elongated oval, widest behind mid-length of elytra, moderately convex dorsally, with the highest point at anterior third of elytral length (lateral view). Colouration black, except reddish-brown mouthparts, antennal clubs, tarsi, claws, trochanters, and ventral portions of femora. Tibiae and remainder of femoral surface dark brown to black. Dorsal pubescence consists mainly of short, thin decumbent yellowish setae arising from small punctures. Plastron microscales (Fig. 7B) on the entire cranium, on pronotum in two lateral bands, covering ca 0.2 of pronotal width on each side, and on the entire surface of elytra. Ventral surface with dense, thin plastron hair-like setae (Fig. 7C) except for prosternal process and median part of metaventrite.

Head. Dorsally entirely covered with plastron scales and with round, setiferous punctures; puncture diameter ca 0.75× diameter of an eye facet, and their distance varies between 0.50–1.00× of a facet diameter. Labrum transverse, with anterior margin straight; anterolateral angles rounded; exposed portion microreticulate, with small setiferous punctures; two types of hair-like setae present, short decumbent setae on most of the surface, and several longer semi-erect setae in a hardly discernible transverse row near mid-length (Fig. 6A), setae nearly half as long as ID and more obvious in males (in older material

Fig. 5. Habitus. **A**. *Elmomorphus brevicornis* Sharp, 1888, ♂, length (anterior margin of clypeus to elytral apex): 3.7 mm (JKCB). **B**. *Elmomorphus amamiensis* Nomura, 1959, ♂, length (anterior margin of clypeus to elytral apex): 3.4 mm (JKCB).
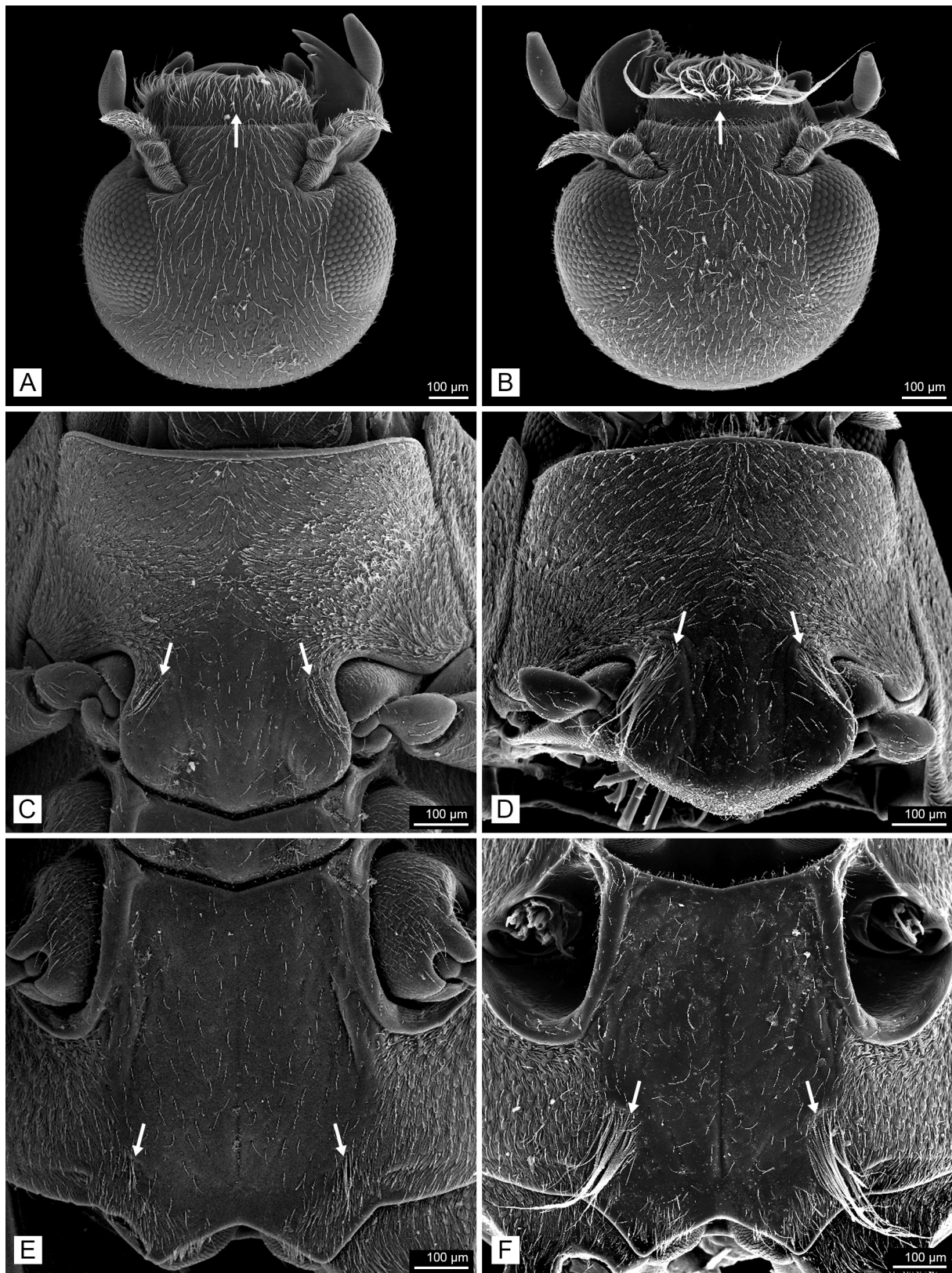
Fig. 6. Details of the male head and ventral portions. **A, C, E**. *Elmomorphus brevicornis* Sharp, 1888 (JKCB). **B, D, F.** *Elmomorphus amamiensis* Nomura, 1959 (JKCB). **A–B**. Head. **C–D**. Ventral view of the prothorax. **E–F**. Ventral view of the metathorax. Arrows show the position of setal clusters.

long setae often abraded). Clypeus with anterior margin straight and with a row of the fine short hairs. Eyes oval, protruding and large, interfacetal setae short; ID: ♂♂ 0.38–0.43 mm (0.41 ± 0.02, n = 14), ♀♀ 0.42–0.48 mm (0.44 ± 0.02, n = 7); APD/ID: ♂♂ 1.93–2.09 (2.01 ± 0.04, n = 14), ♀♀ 1.89–2.04 (1.96 ± 0.05, n = 7). Antennae short, reaching slightly behind middle of eyes, 10-segmented; densely covered by plastron; each club segment with a conspicuous peg-like sensillum on anterior face and numerous hair-like, peg-like and branched sensilla; scape and pedicel small and subequal in length, not enlarged.

THORAX. Pronotum transverse, widest at base, strongly convex, PW/PL: ♂♂ 1.60–1.85 (1.72 ± 0.07, n = 14), ♀♀ 1.60–1.76 (1.68 ± 0.05, n = 7); plastron in lateral band on each side along entire pronotal length, mesally reaching level of third elytral row; disc smooth, shiny, with large round setiferous punctures,
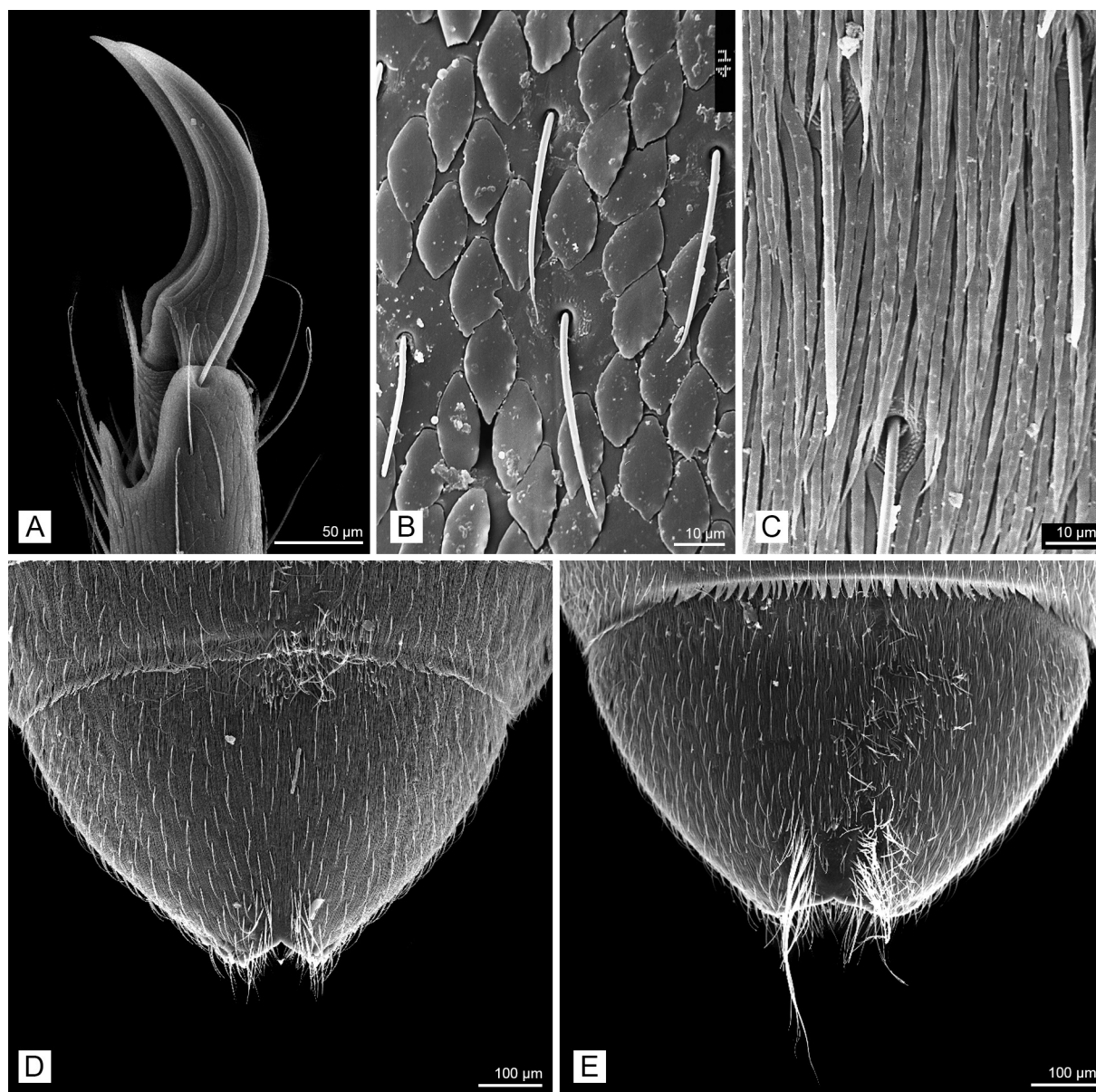
Fig. 7. A–D. *Elmomorphus brevicornis* Sharp, 1888, ♂ (JKCB). **A**. Foreclaws. **B**. Dorsal plastron scales. **C**. Ventral plastron scales. **D**. Detail on ventrite 5. **E**. *Elmomorphus amamiensis* Nomura, 1959, detail on male ventrite 5 (JKCB).

111

punctures nearly as large as facets, separated by 0.50–1.00× of a facet diameter; punctures on plastron area smaller, similar to those on head. Anterior angles strongly deflexed, protruding and acute, third as long as interocular distance; pronotal sides convergent anteriad, distinctly arcuate near middle, moderately explanate along entire length. Hypomeron widest behind mid-length. Prosternal process wide and short, lateral margins divergent and moderately arcuate; posterior margin widely rounded; lateral portion raised, wide and in male with group of longer setae (Fig. 6C) forming a hardly discernible setal cluster (these setae only moderately longer than other hair-like ventral setae and often abraded); median keel moderately convex, ca ⅓ as wide as width of prosternal process. Scutellum longer than wide, smooth, with small, sparse punctures. Metaventral process with lateral sides strongly raised, anterior margin not raised. Metaventral disc flat in female, finely depressed in male; longitudinal step-like elevation along sides delimits lateral area with plastron from smooth central one, surface irregularly and moderately sparsely punctate and in some specimens finely irregularly wrinkled; discrimen well impressed, distinct; a small, hardly discernible setal cluster present in front of metakatepisternal suture in males on each side of metaventral disc (Fig. 6E). Elytra oblong, widest behind middle; moderately convex dorsally, in dorsal view with the highest point at anterior third; sides subparallel in anterior half, more strongly arcuate in posterior half; EL/EW: ♂♂ 1.53–1.69 (1.57 ± 0.04, n = 14), ♀♀ 1.53–1.66 (1.61 ± 0.04, n = 7); surface entirely covered by plastron scales and with numerous minute punctures distinctly smaller than a facet diameter, punctures separated by about 0.50–1.00× a facet diameter. Strial punctures large and deep on elytral disc and subequal in size with facet size, laterad and posteriad progressively smaller. All tibiae straight, to slightly bent near mid-length; protibia ca 1.25× as long as protarsus; PrTL/PL: ♂♂ 1.01–1.20 (1.10 ± 0.05, n = 14), ♀♀ 1.00–1.08 (1.05 ± 0.03, n = 7). Terminal tarsomere in male foreleg ca 1.20× as long as all preceding tarsomeres combined; male foreclaws strongly curved, not widened or thickened, about half of terminal tarsomere length, both similar to each other (Fig. 7A) and similar to female foreclaws.

Abdomen. All ventrites completely covered with plastron; ventrites 1–5 with a length ratio about 1.00: 0.76: 0.60: 0.40: 1.26 in male, and 1.00: 0.90: 0.73: 0.60: 1.60 in female; intercoxal process wide, about twice as wide as long, subtriangular, sides moderately arcuate; admedian keels feebly raised, reaching posterior margin of ventrite. Male ventrite 5 near anterior margin declivous and then shortly flattened, laterad and posteriad evenly deflexed; apex with distinct triangular excision (Fig. 7D); several longer semi-erect setae on each side of excision in hardly discernible clusters. Female ventrite 5 evenly convex and not flattened anteriorly, with minute longitudinal smooth keel at apex and few longer setae alongside keel; apex rounded. Sternite VIII moderately sclerotized laterally, membranous medially, in males with short strut on anterior margin (Fig. 8E), in females with strut almost as long as abdomen (Fig. 9A). Male sternite IX narrow, with sclerotized anterior strut (Fig. 8F). Aedeagus: phallobase long, narrow, expanded proximally (Fig. 8A), PhL/PrL: 2.14–2.36 (2.24 ± 0.07, n = 11); parameres slightly curved ventrad along apical half, nearly straight, with apices narrowly rounded (Fig. 8B); apex of penis slightly expanded and rounded in lateral aspect, not reaching apex of parameres; ventral sclerotized fibula absent. Ovipositor heavily sclerotized; right coxite ca 1.40× as long as left one; paraproct ca 1.80× as long as right coxite (Fig. 9B). Bursa copulatrix with a cluster of numerous minute spines arranged on each side of distal portions (Fig. 9D). Spermatheca tubular; accessory gland large, semi-tubular.

Sexual dimorphism

Females are, on average longer and broader than males. For an unambiguous distinction between males and females, the apex of the fifth ventrite should be examined: it is distinctly excised in males (Fig. 7D), while it is rounded, with a short, smooth keel in females. The presence of several longer semi-erect setae on the labrum, prosternal process, metaventral disc and on the apex of the fifth ventrite in males is hard to observe even in well-preserved specimens, and even under a high-quality microscope at a magnification of about 100×.
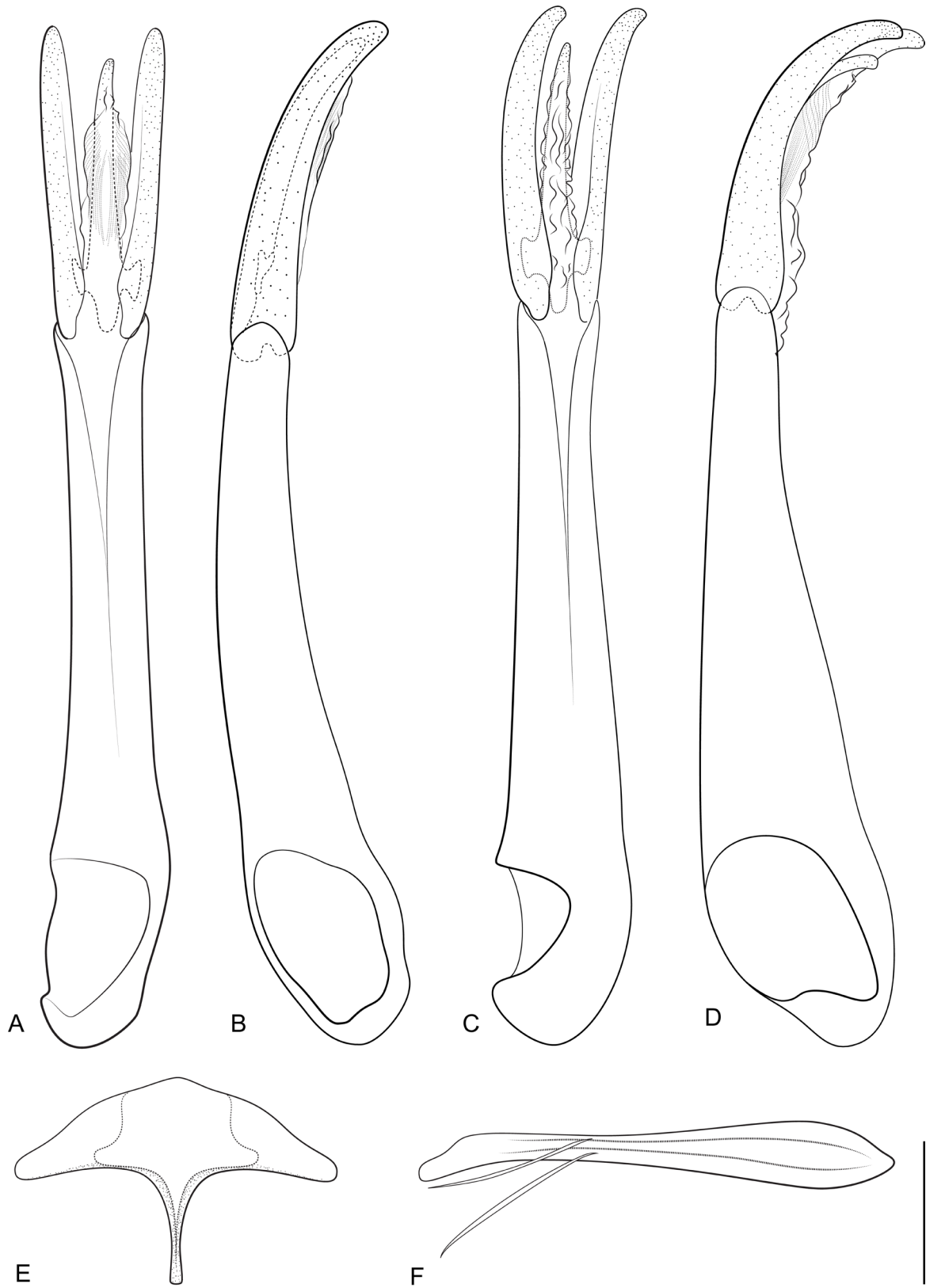
Fig. 8. Male terminalia. **A–B, E–F**. *Elmomorphus brevicornis* Sharp, 1888 (JKCB). **A**. Aedeagus, ventral aspect. **B**. Ibidem, lateral aspect. **C–D**. *Elmomorphus amamiensis* Nomura, 1959 (JKCB). **C**. Aedeagus, ventral aspect. **D**. Ibidem, lateral aspect. **E**. Sternite VIII. **F**. Sternite IX. Scale bar = 0.1 mm.

Distribution

Japan: Honshu, Izu-Ôshima, Oki, Shikoku, Kyushu, Tsushima, and Tanegashima (Nakajima *et al.* 2020); South Korea (Fig. 10A).

Devi *et al*. (2016) erroneously recorded *E. brevicornis* from India. Their record was published in the unreviewed "*Journal of Entomology and Zoology Studies*", a so-called predatory journal (see https://predatoryjournals.com/journals/). The "redescription" provided in this article does not allow any conclusions to be drawn on the identity of the specimens. The "Aedagues" [sic] depicted in their fig. 1c is, in fact, an ovipositor! Judging from their habitus photograph (fig. 1a), these specimens, beyond any doubt, do not belong to *E. brevicornis* or any other species similar to *E. brevicornis.*

Immature stages

The larva was described by Hayashi & Kadowaki (2008) and Hayashi (2015). It was found in a river on submerged roots of *Salix* L. and *Carex* L. (Hayashi pers. com.).

Elmomorphus amamiensis Nomura, 1959
Figs 5B, 6B, D, F, 7E, 8C–D, 9C, E, 10B

Elmomorphus brevicornis amamiensis Nomura, 1959: 33 (original description).

Elmomorphus brevicornis amamiensis – Satô 1960: 252; 1965: 90; 1977: 1. — Kodada & Jäch 2006: 442 (catalogue).
Elmomorphus amamiensis – Jung & Bae 2014: 5 (new status, distribution). — Kodada & Jäch 2016: 606 (catalogue). — Nakajima *et al*. 2020: 178, 322 (diagnosis, identification key, photographs of living specimens).

Type locality

Amami Island, Ryukyu Archipelago, Japan.

Type material (not examined)

See Jung & Bae (2014: 5).

Material examined

JAPAN • 1 ♂; "Amami-Ôshima Shinmura | 13. VI. 1962 M. Sato"; NHMW • 1 ♂; "(Ryukyus) Yona Okinawa 13.VIII.1969 Y. Hori leg."; NHMW • 1 ♂; "Nago-shi, Okinawa-ken 2-5.VIII.1980 Col. K. Baba | *Elmomorphus brevicornis amamiensis* Nomura Det. M. Sato 1992"; NHMW • 4 ♂♂, 4 ♀♀; "Shinokawa, Setouchi-cho, Amami-Ôshima, Kagoshima, Japan, 28.22513, 129.29986, 5.III.2020, H. Yoshitomi leg."; JKCB.

Diagnosis

Elmomorphus amamiensis is medium-sized (TL 2.80–3.22 mm), elongated oval, dorsally moderately convex, with the highest point slightly before the middle of the elytral length (lateral view); body outline slightly discontinuous between pronotum and elytra; plastron microscales covering the entire surface of the cranium, lateral portions of the pronotum and the whole dorsal surface of the elytra (Fig. 5B). Elytron with nine rows of moderately large, round punctures in shallow striae. Legs long and robust, somewhat shorter than the combined length of pronotum and elytra, claws moderately curved. Differences to the morphologically most similar *E. brevicornis* are discussed above.

Measurements (mm)

TL: ♂♂ 2.80–2.99 (2.91 ± 0.06, n = 9), ♀♀ 3.09–3.22 (3.16 ± 0.05, n = 7); PL: ♂♂ 0.68–0.77 (0.74 ± 0.03, n = 9), ♀♀ 0.70–0.78 (0.76 ± 0.03, n = 7); PW: ♂♂ 1.14–1.24 (1.20 ± 0.03, n = 9), ♀♀ 1.25–1.35 (1.31 ± 0.03, n = 7); EL: ♂♂ 2.18–2.34 (2.27 ± 0.05, n = 9), ♀♀ 2.42–2.60 (2.50 ± 0.05, n = 7); EW: ♂♂ 1.38–1.46 (1.42 ± 0.02, n = 9), ♀♀ 1.48–1.59 (1.54 ± 0.04, n = 7); MsTL: ♂♂ 0.84–0.96 (0.92 ± 0.03, n = 9), ♀♀ 0.83–0.87 (0.85 ± 0.01, n = 7); MtTL: ♂♂ 1.03–1.10 (1.07 ± 0.03, n = 9), ♀♀ 0.99–1.04 (1.02 ± 0.02, n = 7); PhL: 0.91–1.19 (1.02 ± 0.08, n = 7); PrL: 0.39–0.43 (0.42 ± 0.01, n = 7).

Redescription

Body. Elongated oval, widest behind mid-length of elytra, moderately convex dorsally. Colouration black; mouthparts, antennae, tibiae and tarsi reddish-brown; femora dark brown. Main pubescence consisting of very short and thin, decumbent yellowish setae, which arise from small punctures. Dorsal plastron present on the entire surface except for the pronotal disc. Ventral surface except for prosternal process and disc of metaventrite with hair-like plastron setae.

Head. With plastron and round setiferous punctures with a diameter of ca 0.75× a facet diameter, punctures separated by distance 0.50–1.00× a facet diameter. Labrum transverse, anterior margin straight, setose; anterolateral angles rounded; exposed portion microreticulate and micropunctate; male with a transverse row of strong, densely set conspicuous setae near middle (Fig. 6B), longest setae laterally, in
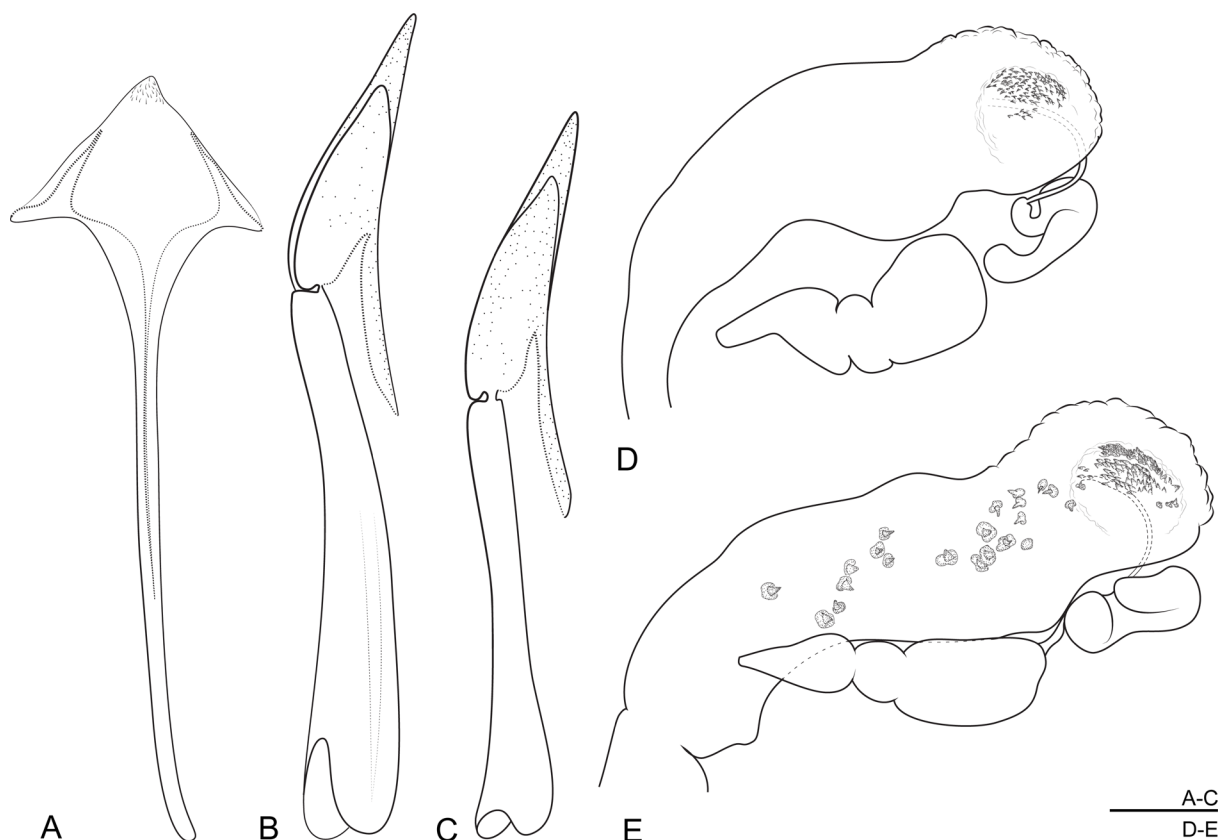
Fig. 9. Female terminalia. **A–B, D**. *Elmomorphus brevicornis* Sharp, 1888 (JKCB). **A**. Sternite VIII. **B**. Ovipositor. **C, E**. *Elmomorphus amamiensis* Nomura, 1959 (JKCB). **C**. Ovipositor. **D**. Bursa copulatrix. **E**. Bursa copulatrix. Scale bars = 0.1 mm.

length subequal to two-third of interocular distance; female with shorter and rather sparse setae, setal row hardly discernible. Anterior margin of clypeus straight, and not in the same plane as labrum. Eyes large, oval, protruding; interfacetal setae sparse, short; ID: ♂♂ 0.37–0.43 mm (0.40 ± 0.02, n = 9), ♀♀ 0.43–0.48 mm (0.44 ± 0.02, n = 7). Antennae 10-segmented, shorter than eye length.

THORAX. Pronotum transverse, moderately convex, widest at base, PW/PL: ♂♂ 1.60–1.71 (1.62 ± 0.04, n = 9), ♀♀ 1.66–1.91 (1.73 ± 0.08, n = 7); plastron on entire lateral portions, mesally reaching level of third elytral row; pronotal disc smooth, with large, round setiferous punctures; punctures slightly smaller than facets, nearly regularly spaced, interstices 0.75–1.20× a facet diameter. Anterior angles strongly protruding, acute and deflexed; lateral sides of pronotum convergent anteriad, slightly arcuate or nearly straight, narrowly explanate. Prosternal process with lateral margins divergent, moderately arcuate; posterior margin rounded; lateral portion slightly elevated, separated from median keel by longitudinal depressions; median keel nearly flat, surface finely punctate and irregularly wrinkled. Male with two clusters of conspicuous long setae in anterolateral portions of prosternal process (Fig. 6D), longest setae as long as prosternum in front of prosternal process. Scutellum longer than wide, surface smooth, with small, sparse punctures. Metaventrite along middle ca twice as long as prosternal process; disc flat in males, slightly elevated in females, discrimen present nearly along the entire length, surface finely sparsely punctate, and irregularly wrinkled. Metaventral process as long as prosternal one, with lateral sides keel-like, anterior margin not straight, flat; male with two clusters of conspicuous long setae in posterolateral portions of metaventrite (Fig. 6F). Elytra ovate, widest behind middle; sides moderately arcuate, more convergent posteriad than anteriad, narrowly explanate; EL/EW: ♂♂ 1.57–1.64 (1.60 ± 0.02, n = 9), ♀♀ 1.57–1.65 (1.62 ± 0.02, n = 7); entire surface with plastron; each elytron with nine striae, strial punctures smaller than facets, separated by distance of 1.00–2.00× puncture diameter; punctures smaller laterad and toward apex. Tibiae all straight, slender; protibia ca 1.25× as long as protarsus; PrTL/PL: ♂♂ 1.12–1.25 (1.19 ± 0.04, n = 9), ♀♀ 1.03–1.21 (1.09 ± 0.05, n = 7). Terminal protarsomere in male ca 1.20× as long as all preceding tarsomeres combined; male foreclaws moderately curved, not widened or thickened, slightly less than half length of the terminal tarsomere length, both similar to each other and similar to female foreclaws.

ABDOMEN. Ventrites completely covered with plastron; ventrites 1–5 with length ratio 1.00: 0.74: 0.52: 0.48: 1.66 in male, and 1.00: 0.88: 0.65: 0.57: 1.84 in female. Intercoxal process wide, about twice as wide as long, subtriangular, sides distinctly arcuate; admedian keels indistinct, feebly raised in male, reaching posterior margin of ventrite, but nearly absent in female. Mesal portion of male ventrite 5 flattened on anterior third and strongly deflected posteriad (lateral view); apex with distinct triangular excision and cluster of several long semi-erect setae on each side of excision (Fig. 7E). Female ventrite 5 evenly convex and only indistinctly flattened anteriorly, with minute longitudinal smooth keel at apex and few longer setae alongside keel; apex rounded. Aedeagus: phallobase long, narrow, expanded proximally (Fig. 8C), PhL/PrL: 2.32–2.74 (2.43 ± 0.12, n = 7); parameres strongly curved ventrad, especially in apical half (Fig. 8D), moderately narrowed, apices subacute; penis with apex slightly expanded and rounded in lateral aspect; sclerotized fibula absent. Ovipositor heavily sclerotized; right coxite ca 1.30× as long as left one; paraproct ca 1.52× as long as right coxite (Fig. 9D). Bursa copulatrix with cluster of minute spines on each side of distal portions and with several larger sclerites scattered over proximal portion (Fig. 9E).

Sexual dimorphism

Females are on average larger than males, and the apex of their fifth ventrite is rounded, while in males it is triangularly excised. Moreover, males have long conspicuous setae arranged in a transverse row on the labrum and in clusters situated on lateral sides of the prosternal process, lateral sides of the metaventrite and on the apex of the fifth ventrite; females lack these groups of long setae.

Distribution

Elmomorphus amamiensis has been so far recorded only from the Ryukyu Archipelago in Japan (Fig. 10B): Amami Island, Tokunoshima, Okinawa-jima, Iheya-jima, Zamami-shoto, Aka-jima, and Kume-jima (Nakajima *et al.* 2020).

Key to the adults of the species of Elmomorphus from Japan and Korea

1. Male labrum with several long, rather widely spaced setae arranged in a more or less distinct transverse row (Fig. 6A); similar, moderately longer setae arranged in small clusters on prosternal process and metaventrite (Fig. 6C, E), and on apex of ventrite 5 (Fig. 7D); long setae on labrum maximally half as long as interocular distance, most elongate ventral setae moderately shorter than those on labrum. Parameres in apical half slightly curved ventrad, nearly straight (Fig. 8B). Female: bursa copulatrix with a cluster of minute spines on each side in distal portions (Fig. 9D) ....*E. brevicornis* Sharp, 1888
– Male labrum with numerous conspicuously long, closely arranged setae in a transverse row (Fig. 6B); similar setae in extensive clusters on prosternal process, metaventrite (Fig. 6D, F), and on apex of ventrite 5 (Fig. 7E); most elongate setae on labrum about ⅔ of interocular distance, longest ventral setae moderately longer than interocular distance. Parameres in apical half strongly curved (Fig. 8D). Female: bursa copulatrix with cluster of minute spines and with several larger sclerites scattered over its proximal portion (Fig. 9E) ....*E. amamiensis* Nomura, 1959

Discussion

Elmomorphus brevicornis has been recorded on six Japanese islands and has been quite recently, discovered in South Korea (Jung & Bae 2014; Nakajima *et al.* 2020). Interestingly, an extensive collection of *Elmomorphus* specimens sampled during the China Water Beetle Survey from several hundred Chinese localities, including Taiwan, did not contain any specimens of *E. brevicornis*. Similarly, there have been no records from the Russian Far East, Vietnam, Laos, or Thailand. Therefore, *E. brevicornis* was for a long time considered to be an endemic species of Japan (Kodada & Jäch 2006).
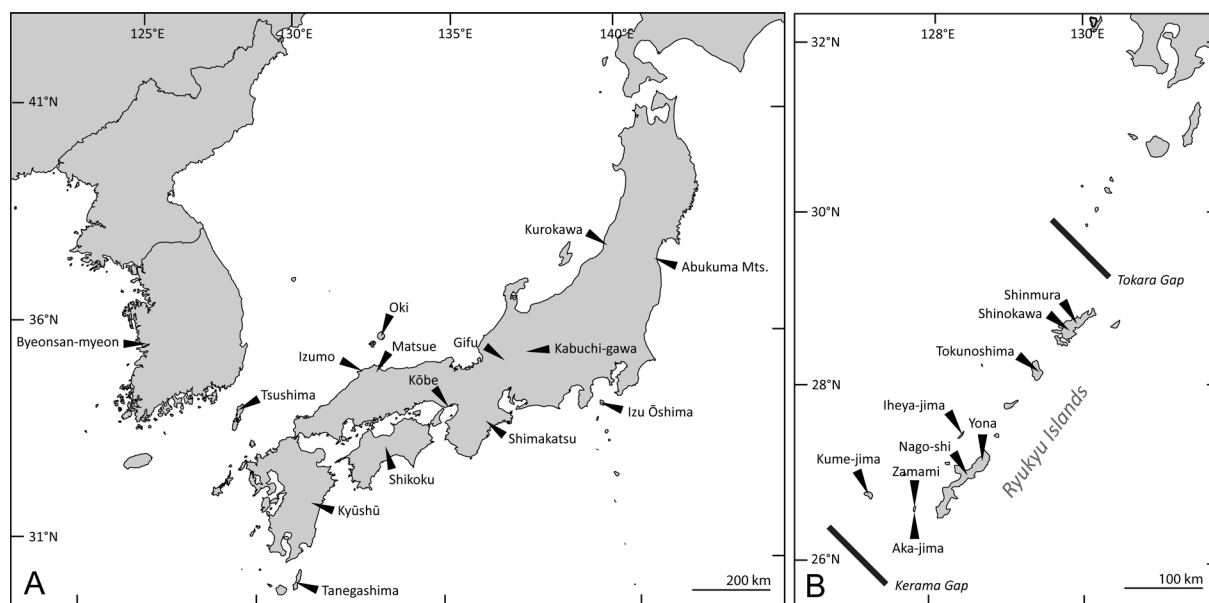

Fig. 10. Map showing records of **A**. *Elmomorphus brevicornis* Sharp, 1888. **B**. *Elmomorphus amamiensis* Nomura, 1959.

The subspecies *E. brevicornis amamiensis* was established based on a female holotype collected on Amami-Ôshima, one of the largest islands of the Ryukyu Archipelago (Nomura 1959).

Jung & Bae (2014) examined specimens of *E. brevicornis* from Korea and *E. brevicornis amamiensis* from Amami Island. Using differences in the structure of the male genitalia, they raised the subspecies *amamiensis* to species level. In their identification key, *E. amamiensis* was characterized by the long mesofemur, tarsi and claws small, and parameres strongly curved apically; while *E. brevicornis* possesses a shorter mesofemur, large tarsi and claws, and parameres, which are not strongly curved apically (Jung & Bae 2014: 7).

The present principal component analysis classified males of the two species of *Elmomorphus* in two homogenous groups that were separated along the first ordination axis given the eight morphometric characters studied. The pronotal length and width are strongly correlated with PC1, while the length of meso- and metatibia are correlated with PC2. This corresponds well to raw measurements according to which the average body size of *E. amamiensis* males is smaller, while the average tibial length of *E. brevicornis* males is higher than in *E. amamiensis*. Although the average values are comparatively different, the ranges of individual characters overlap in the two species. Individual characters thus do not allow unambiguous species identification. However, the combination of eight morphometric features can differentiate males of the two species without any overlap in the phenotypic space. Females of the two species were only vaguely separated along the first ordination axis, as two specimens of *E. brevicornis* were placed within the relatively compact cluster of *E. amamiensis* individuals. The present multivariate analyses show that females of the two species cannot be unambiguously differentiated even when a combination of eight morphometric characters is considered. Nevertheless, we cannot exclude that inclusion of a significantly larger number of individuals from a wider distributional area into multivariate analyses might bring moderately different results. So far, the best characters for species identification of males are the conspicuous long hair-like setae on the labrum, prosternal process, metaventrite, and on the fifth ventrite in combination with the specific form of the parameres. Females can be distinguished by the different patterns of various sclerites on the bursa copulatrix.

Contrary to the morphological similarity between the two species, the present barcoding analyses show a profound interspecific divergence of *E. amamiensis* and *E. brevicornis* and confirm their species status as proposed by Jung & Bae (2014). In addition, the haplotype network analyses supported the monophyletic origin of *E. amamiensis* and *E. brevicornis* by 55 shared nucleotide positions within the barcoding COI sequence fragment, although the two species differ in 109 nucleotide positions. This deep interspecific divergence is in congruence with the different geographic distribution of the two species. *Elmomorphus amamiensis* is confined to the Ryukyu Archipelago and has so far not been recorded north of the Watase Line (Tokara gap), a biogeographical barrier between the Holarctic and the Oriental regions, nor has it been found south of the Miyako Strait (Kerama gap) south of Okinawa. Thus, *E. amamiensis* represents one of the numerous endemic species of the Ryukyu Archipelago. On the other hand, *E. brevicornis* occurs north of the Tokara gap on several Japanese islands and in South Korea. The deep divergences within the COI sequences of the two *Elmomorphus* species suggest their different evolutionary origin rather than their sister-group relationship.

Acknowledgements

References

Bollow H. 1940. Monographie der palaearktischen Dryopidae mit Berücksichtung der eventuell transgredierenden Arten (Col.). *Mitteilungen der Münchner Entomologischen Gesellschaft* 30 (1): 24–71.

Chûjô M. & Satô M. 1964. Family Dryopidae. *In*: Kira T. & Umesao T. (eds) *Nature and Life in Southeast Asia. Volume III*: 193–194. Fauna and Flora Research Society, Kyoto.

Clement M., Posada D. & Crandall K.A. 2000. TCS: a computer program to estimate gene genealogies. *Molecular Ecology* 9 (10): 1657–1659. https://doi.org/10.1046/j.1365-294x.2000.01020.x

Darriba D., Taboada G.L., Doallo R. & Posada D. 2012. jModelTest 2: more models, new heuristics and parallel computing. *Nature Methods* 9 (8): 772. https://doi.org/10.1038/nmeth.2109

Delève J. 1968. Dryopidae et Elminthidae (Coleoptera) du Vietnam. *Annales Historico-Naturales Musei Nationalis Hungarici* 60: 149–181.

Devi M.B., Devi O.S. & Wanghengbam L. 2016. Redescription of the first record of the species *Elmomorphus brevicornis* from the family Dryopidae (Coleoptera) in Manipur. *Journal of Entomology and Zoology Studies* 4 (3): 371–373.

Folmer O., Black M., Hoeh W., Lutz R. & Vrijenhoek R. 1994. DNA primers for amplification of mitochondrial cytochrome c oxidase subunit I from diverse metazoan invertebrates. *Molecular Marine Biology and Biotechnology* 3 (5): 294–299.

Hammer Ø., Harper D.A.T. & Ryan P.D. 2001. PAST: Paleontological statistics software package for education and data analysis. *Palaeontologia Electronica* 4 (1): 1–9. http://palaeo-electronica.org/2001_1/past/issue1_01.htm

Hayashi M. 2011. Aquatic Coleoptera of Shimane Prefecture. *Special Bulletin of the Hoshizaki Green Foundation* 1: 1–117.

Hayashi M. 2015. Description of larva of *Elmomorphus brevicornis* Sharp (Coleoptera, Dryopidae). *Bulletin of the Hoshizaki Green Foundation* 18: 219–223. [In Japanese with English abstract.]

Hayashi M. & Kadowaki H. 2008. Records on aquatic Coleoptera from rivers in and around Mt. Daisen, Tottori Prefecture, Japan, part II. *Bulletin of the Hoshizaki Green Foundation* 11: 269–286. [In Japanese with English abstract.]

Hayashi M. & Shimada T. 2006. Records on Elmidae and Dryopidae from Eastern Area of Shimane Prefecture and Oki Islands, Japan. *Bulletin of the Hoshizaki Green Foundation* 9: 127–143. [In Japanese with English abstract.]

Hebert P.D.N., Cywinska A., Ball S.L. & deWaard J.R. 2003. Biological identifications through DNA barcodes. *Proceedings of the Royal Society B, Biological Sciences* 270 (1512): 313–321. https://doi.org/10.1098/rspb.2002.2218

Hoang D.T., Chernomor O., von Haeseler A., Minh B.Q. & Vinh L.S. 2018. UFBoot2: improving the ultrafast bootstrap approximation. *Molecular Biology and Evolution* 35 (2): 518–522. https://doi.org/10.1093/molbev/msx281

Hunter J.D. 2007. Matplotlib: a 2D graphics environment. *Computing in Science and Engineering* 9: 90–95. https://doi.org/10.1109/MCSE.2007.55

ICZN 1999. *International Code of Zoological Nomenclature. Fourth Edition*. International Trust for Zoological Nomenclature, London.

Jäch M.A. 1984. Die Koleopterenfauna der Bergbäche von Südwest-Ceylon (Col.). *Archiv für Hydrobiologie Supplement* 69 (2): 228–332.

Jäch M.A. 1998. Annotated check list of aquatic and riparian/littoral beetle families of the world (Coleoptera). *In*: Jäch M.A. & Ji L. (eds) *Water Beetles of China, Volume II*: 25–42. Zoologisch-Botanische Gesellschaft in Österreich und Wiener Coleopterologenverein, Vienna.

Jäch M.A. & Balke M. 2008. Global diversity of water beetles (Coleoptera) in freshwater. *In*: Balian E.V., Levéque C., Segers H. & Martens K. (eds) Freshwater Animal Diversity Assessment. *Hydrobiologia* 595 (1): 419–442. https://doi.org/10.1007/s10750-007-9117-y

Jung S.W. & Bae Y.J. 2014. First record of the family Dryopidae (Coleoptera) in Korea with taxonomic notes on *Elmomorphus brevicornis* and *Elmomorphus amamiensis*. *Animal Systematics, Evolution and Diversity* 30 (1): 1–8. https://doi.org/10.5635/ASED.2014.30.1.001

Kamezawa H. & Nomura S. 2013. Records of *Elmomorphus brevicornis* Sharp from Izu-Oshima, Izu Islands, Japan. *Sabyabane, New Series* 9: 29. [In Japanese.]

Kodada J. & Jäch M.A. 2006. Family Dryopidae Billberg, 1820. *In*: Löbl I. & Smetana A. (eds) *Catalogue of Palaearctic Coleoptera. Volume 3. Scarabaeoidea, Scirtoidea, Dascilloidea, Buprestoidea, Byrrhoidea*: 441–443. Apollo Books, Stenstrup.

Kodada J. & Jäch M.A. 2016. Family Dryopidae Billberg, 1820 (1817). *In*: Löbl I. & Löbl D. (eds) *Catalogue of Palaearctic Coleoptera. Volume 3. Revised and updated edition. Scarabaeoidea, Scirtoidea, Dascilloidea, Buprestoidea and Byrrhoidea*: 603–607. Brill, Leiden / Boston.

Kodada J., Jäch M.A. & Čiampor F. 2016. 19.3. Dryopidae Bilberg, 1820 (1817). *In*: Beutel R.G. & Leschen R.A.B. (eds) *Coleoptera, Beetles. Volume 1: Morphology and Systematics (Archostemata, Adephaga, Myxophaga, Polyphaga partim), Handbook of Zoology, Arthropoda: Insecta*: 590–602. 2nd Ed. Walter de Gruyter, Berlin.

Kôno H. 1934. Die Dryopiden aus Japan. *Insecta Matsumurana* 8 (3): 124–128.

Kumar S., Stecher G., Li M., Knyaz C. & Tamura K. 2018. MEGA X: Molecular Evolutionary Genetics Analysis across computing platforms. *Molecular Biology and Evolution* 35 (6): 1547–1549. https://doi.org/10.1093/molbev/msy096

Leigh J.W. & Bryant D. 2015. POPART: full-feature software for haplotype network construction. *Methods in Ecology and Evolution* 6 (9): 1110–1116. https://doi.org/10.1111/2041-210X.12410

Lewis G. 1879. *A Catalogue of Coleoptera from the Japanese Archipelago*. Taylor and Francis, London.

Miller M.A., Pfeiffer W. & Schwartz T. 2010. Creating the CIPRES Science Gateway for inference of large phylogenetic trees. *In*: *Proceedings of the Gateway Computing Environments Workshop (GCE)*: 1–8. IEEE, New Orleans, Louisiana. https://doi.org/10.1109/GCE.2010.5676129

Nakajima J., Hayashi M., Ishida K., Kitano T. & Yoshitomi H. 2020. Dryopidae. In: *Aquatic Coleoptera and Hemiptera of Japan*: 177–179. Bun-ichi Sogo Shuppan, Tokyo. [In Japanese.]

Nguyen L.-T., Schmidt H.A., Haeseler A. von & Minh B.Q. 2015. IQ-TREE: a fast and effective stochastic algorithm for estimating maximum-likelihood phylogenies. *Molecular Biology and Evolution* 32 (1): 268–274. https://doi.org/10.1093/molbev/msu300

Nomura S. 1959. Notes on the Japanese Dryopoidea (Coleoptera) II. *Tôhô-Gakuhô* 9: 33–38, 1 pl.

Pedregosa F., Varoquaux G., Gramfort A., Michel V., Thirion B., Grisel O., Blondel M., Prettenhofer P., Weiss R., Dubourg V., Vanderplas J., Passos A., Cournapeau D., Brucher M., Perrot M. & Duchesnay É. 2011. Scikit-learn: machine learning in Python. *Journal of Machine Learning Research* 12: 2825–2830.

Ronquist F., Teslenko M., Mark P. van der, Ayres D.L., Darling A., Höhna S., Larget B., Liu L., Suchard M.A. & Huelsenbeck J.P. 2012. MrBayes 3.2: efficient Bayesian phylogenetic inference and model choice across a large model space. *Systematic Biology* 61 (3): 539–542.
https://doi.org/10.1093/sysbio/sys029

Satô M. 1960. Aquatic Coleoptera from Amami-Ôshima of the Ryukyu Islands (I). *Kontyû* 28 (4): 251–254.

Satô M. 1965. Dryopoidea of the Ryukyu Archipelago, I (Coleoptera). *Journal of the Nagoya Women's College* 11: 76–94.

Satô M. 1977. Family Dryopidae. *Check-List of Coleoptera of Japan* 8: 1.

Satô M. 1981. Dryopidea (Coleoptera) of Nepal I. Family Dryopidae. *Bulletin of Natural Science Museum Tokyo, Series A (Zoology)* 7 (1): 51–56.

Sharp D. 1888. Descriptions of some new Coleoptera from Japan. *Annals and Magazine of Natural History Series 6* 2: 242–245. https://doi.org/10.1080/00222938809460918

Swan D.C. 1936. Berlese's fluid: remarks upon its preparation and use as a mounting medium. *Bulletin of Entomological Research* 27 (3): 389–391. https://doi.org/10.1017/S0007485300058259

Yoshioka M. 2007. Records on Dryopidae and Elmidae from water systems of Iinashi-gawa and Iu-gawa River, Eastern Area of Shimane Prefecture. *Bulletin of the Hoshizaki Green Foundation* 10: 235–256. [In Japanese with English abstract.]

Yoshioka M. 2008. Records on Dryopidae and Elmidae from water systems of Hakuta-gawa River and Hino-gawa River in San'in District, Japan. *Bulletin of the Hoshizaki Green Foundation* 11: 223–237. [In Japanese with English abstract.]

Yoshitomi H. & Haga K. 2018. A new record of *Dryops nitidulus* (Coleoptera, Dryopidae) from Japan. *Elytra, Tokyo, New Series* 8 (2): 341–342.

Zaitzev P. 1910. Dryopidae, Cyathoceridae, Georyssidae, Heteroceridae. *In*: Schenkling S. (ed.) *Coleopterorum Catalogus* 17: 1–68. W. Junk, Berlin. Available from
https://www.biodiversitylibrary.org/item/189656#page/3/mode/1up [accessed 4 Jun. 2021].